Journal of Materials Chemistry B

PAPER

View Article Online
View Journal | View Issue

Cite this: J. Mater. Chem. B, 2014, 2, 7440

Silica–PEG gel immobilization of mammalian cells†

Eduardo Reátegui,[a] Lisa Kasinkas,[a] Katrina Kniesz,[a] Molly A. Lefebvre[a] and Alptekin Aksan*[ab]

Received 19th May 2014
Accepted 17th September 2014

DOI: 10.1039/c4tb00812j

www.rsc.org/MaterialsB

In this study, human foreskin fibroblasts and mouse embryonic fibroblasts were encapsulated in mechanically reversible, THEOS and THEOS–PEG gels that completely immobilized them restricting their motility, growth and proliferation. The changes in the membrane integrity and metabolic activity (MA) of the immobilized cells were measured by IR spectroscopy and fluorescence microscopy. To explore the effects of surface chemistry and porosity on immobilized cell MA, different amounts of a biocompatible polymer, polyethylene glycol PEG, was incorporated into the silica gels. To explore the effects of the proliferative stress, in selected experiments, cellular proliferation was arrested prior to immobilization by exposing the cells to irradiation. Four main factors were identified that affect the long-term survival of the cells within the immobilization matrix: (1) porosity/permeability of the gel, (2) structural homogeneity of the gel, (3) specific interactions between the cell membrane and the gel surface and (4) the proliferative stress. It was shown that the immobilized cells could easily be mechanically recovered from the gel and upon incubation, proliferated normally. It is believed that the gels and the matrix developed here have very significant potential applications in tissue engineering and in personalized cancer treatment.

Introduction

Eukaryotes have long been encapsulated in alginate, collagen, chitosan, agarose, polyglycolic acid (PGA) or polylactic acid (PLA) based organic gels to be used in biomedical applications such as cell therapy and tissue engineering.[1–6] In general, these organic matrices are highly biocompatible, can be engineered to have architectures mimicking the extracellular matrix, and offer high permeability to nutrients but are mechanically weak. Therefore, exfiltration of the encapsulated cells or infiltration of the gel by other cells is a common occurrence in organic matrices.[7,8] However, the low mechanical compliance of the organic gels provides the encapsulated cells with an environment where high motility, growth and normal proliferation is enabled.[9,10] Inorganic matrices (such as silica gels) on the other hand, are chemically and thermally stable, resistant to cell infiltration and exfiltration, and are mechanically sturdier.[10,11] Silica gels that contain encapsulated prokaryotes have been used as biosensors,[12,13] biocatalysis platforms,[11,14] and bioremediation systems,[15,16] as well as for alternative energy production and CO_2 sequestration purposes.[17,18] However, only a very small number of studies have been conducted with silica gel encapsulated eukaryotes and almost all of these studies have focused on cell therapy applications.[14,19–21]

The earliest report on successful long-term sustained functionality observed in silica encapsulated mammalian cells is with mouse pancreatic islet cells encapsulated in hydrolyzed silica alkoxide precursors.[22] One downside of this approach (not explored in the report) is the decreased viability and function of the cells due to toxicity of ethanol, which is a condensation product of silica gelation. To avoid exposure to ethanol, alkoxide precursors may be volatilized and then condensed onto the surface of the cells to be encapsulated, forming a very thin, stable and homogeneous layer of SiO_2 in a process called the biosil method.[23] It was shown that Hep G2 human cancer cells and human fibroblasts can be viable and functional after biosil encapsulation.[24,25] Other approaches for removing the alcohol formed during hydrolysis of the alkoxides are also used for the encapsulation of clumps or clusters of mouse fibroblasts.[26,27] Water-based precursors such as silica nanoparticles or sodium silicate are proven to be more biocompatible for the encapsulation of HUVEC and hybridoma cells.[27,28] Recently, alkoxide tetrakis(2-hydroxyethyl)orthosilicate (THEOS) gels are shown to provide high level of viability to encapsulated hybridoma cells, allowing functionality for antibody production and release.[28] Hybrid cell encapsulation approaches are also used where cells are first embedded in a polymeric capsule (*e.g.*, alginate) and then covered with a silica shell (*e.g.*, alkoxide or sodium silicate) maintaining the functionality of the eukaryotic cells by isolating them from the silica interface.[19,29,30]

In all of the studies described above (both for organic and inorganic gels), the main aim was to create a synthetic ecosystem where the encapsulated eukaryotes were partially isolated from their immediate environments but continued to

[a]Biostabilization Laboratory, Department of Mechanical Engineering, University of Minnesota, Minneapolis, MN 55455, USA. E-mail: aaksan@umn.edu

[b]BioTechnology Institute, University of Minnesota, Minneapolis, MN 55455, USA

† Electronic supplementary information (ESI) available. See DOI: 10.1039/c4tb00812j

live and function normally. In this paper, we developed a porous yet stiff silica gel that completely inhibited the motility, growth and proliferation of the encapsulated mammalian cells. Furthermore, after encapsulation, the cells could be released, on demand, by mechanical agitation. The stiff gel immobilization technology and the on demand release method were developed to explore if mammalian cells could survive these conditions and to explore the main factors that determine their survival in the immobilized state. In encapsulated prokaryotes for example, significantly enhanced metabolic activity was reported if proliferation was completely inhibited.[31–33] To date, no such study has been conducted with eukaryotes.

In this study, human foreskin fibroblasts (HFF) and mouse embryonic fibroblasts (MEF) were encapsulated in 3D pure THEOS and THEOS–PEG gels that completely immobilized them restricting their motility, growth and proliferation. The changes in the membrane integrity and metabolic activity (MA) of the immobilized cells were measured by IR spectroscopy and fluorescence microscopy in gels of different structure, porosity, and surface chemistry. To explore the effects of surface chemistry and porosity, different amounts of a biocompatible polymer, polyethylene glycol (PEG), was incorporated into the silica gels. To explore the effects of the proliferative stress, in selected experiments, cellular proliferation was arrested prior to immobilization by exposing the cells to irradiation.

Materials and methods

Tetrakis(2-hydroxyethyl)orthosilicate (THEOS) was purchased from Gelest Inc. (Morrisville, PA). 85 nm diameter colloidal silica nanoparticles (SNPs) were obtained from NYACOL Nano Technologies Inc. (Ashland, MA). SNPs were purified using dialysis through a 3.5 kDa cut-off membrane. Linear polyethylene glycol (PEG) at molecular weights of $M_w = 0.4$, and 0.6 kDa were purchased from Sigma-Aldrich Corp. (St. Louis, MO); and 4-arm PEG ($M_w = 2$ kDa) was purchased from Creative PEGWorks (Winston Salem, NC). All chemicals were used without further purification.

Cell culture

Human foreskin fibroblasts (HFF) and mouse embryonic fibroblasts (MEF) were purchased from the American Type Cell Collection (Manasas, VA). HFF and MEF cells were cultured in DMEM basal media supplemented with 15% fetal bovine serum (FBS), and 1% penicillin/streptomycin. The cells were incubated in T75 flaks in a 5% CO_2 atmosphere at 37 °C until they reached 80–90% confluence. Before immobilization, the cells were washed with phosphate buffer saline (PBS) and suspended by exposure to 0.25% trypsin–EDTA for 5 min at 37 °C and pelleted by centrifugation at 800 rpm for 5 min. The supernatant was removed and the cells were re-suspended in growth media at a concentration of ~500 000 cells per mL. In some experiments, before immobilization, the cells were irradiated at a dose of 6000 rads (for HFFs) and 10 000 rads (for MEFs) using an X-ray machine. It was confirmed by plating that the irradiated HFF (HFFIR) and irradiated MEF (MEFIR) cells were alive (at rates of 93.3% and 92.7%, respectively) but stopped proliferating. The dead HFF and MEF cells used in the negative controls were killed by incubating them in 70% ethanol for 10 minutes. The dead cells were then washed and suspended in media. Compromised membrane integrity of the "dead" cells was verified before and after immobilization using fluorescence microcopy (Fig. S1†).

Silica gel synthesis and characterization

Synthesis of the silica gels involved direct hydrolysis of THEOS in cell culture media at 10% (v/v) concentration in the absence of an acid catalyst. 0.01 M 85 nm SNPs was also added to the cell culture medium. The mixture was then stirred vigorously for 60 s. A change in the pH of the mixture as a result of THEOS hydrolysis (~pH 5) was observed as the color of the media turned yellow. The condensation reaction proceeded immediately, leading to the formation of the nanoporous silica matrix. The pH was recovered (~7.4) after the sol–gel transition of the hydrolyzed alkoxide. PEG containing silica gels (SPEG gels) were produced by dissolving PEG in cell culture media, which was then added to the hydrolyzed THEOS solution. The final concentration of PEG in the cell culture media mixture was set to 2.3, 4.5, and 10% (v/v).

Kinetics of formation of the silica and SPEG gels was measured using oscillatory rheometry with an AR-G2 rheometer (TA Instruments, New Castle, DE). Briefly, the experiments were performed using a 2° angle conical plate of 40 mm in diameter with a truncation gap distance of 49 μm. Briefly, 1.5 mL of the experimental solution (*e.g.*, silica sol or SPEG gel) was placed between the plates of the rheometer operating at a constant angular frequency of 1 rad s^{-1} and a strain of 0.05%. The storage (G') and loss (G'') moduli were measured continuously over time through the sol–gel transition. The crossover between G' and G'' corresponded to the gelation time (T_g).

Prepared gels were characterized using Fourier Transform Infrared (FTIR) spectroscopy with a Thermo-Nicolet 6700 Microspectrometer (Thermo Electron Corporation LLC, Waltham, MA). FTIR analysis was conducted to determine the changes in the chemical structure of the gels when PEG was incorporated. UV-vis spectroscopy (Molecular Devices, Sunnyvale, CA) was performed on the gels to detect phase separation. A drop in the transmittance values between 450 to 750 nm was taken to indicate phase separation in the gels. Scanning electron microscopy (SEM) analysis was conducted with a Hitachi S-900 FESEM (Hitachi Co., Lawrenceville, GA). SEM images of the different gels were analyzed to determine the ultrastructural changes in the architecture of the gel and to measure apparent porosity.[34] ImageJ[35] software was used to measure the apparent porosity using at least five images per experimental group.

Cell immobilization

For immobilization in silica gels, 20 μL of 0.01 M SNPs in culture media was mixed with 4 μL of THEOS. The mixture was vortexed for 1 min and was placed on ice to avoid condensation. After the pH recovered to 7.4, 20 μL of cell solution containing 500 000 cell per mL was added to the SNP THEOS solution,

mixed gently with a pipette, and transferred to a 96-well plate. Gelation was completed in 5 min, and 50 μL of media was added on top of the formed gel to avoid drying. The encapsulated cells were then incubated in 5% CO_2 atmosphere at 37 °C (Fig. 1).

For immobilization in SPEG gels, linear (SPEG-l) or 4-arm PEG (SPEG-4arm) was added at concentrations of 2.3%, 4.5%, or 10% (v/v) to 20 μL of 0.01 M SNPs suspended in culture media. The rest of the immobilization procedure was similar to that described above. To granulate the gels prior to immobilization, the gels were sonicated with excess media for 5 min at 30% power. The solution was then centrifuged at 1500 rpm for 5 min and the excess media was removed leaving behind a granulated SPEG gel.

Measurement of cell membrane integrity and lipid conformation

The integrity of the cellular membranes after immobilization in silica and SPEG gels was evaluated using a live-dead fluorescence assay using calcein, Hoechst (H) and propidium iodide (PI) fluorescent dyes. A Nikon Eclipse T200 microscope (Nikon Instruments Inc., Melville, NY) equipped with 10× and 20× objectives were used to collect brightfield and fluorescent images of the encapsulated cells. The change in the cell membrane lipid conformation due to immobilization was quantified by monitoring the wavenumber shift of the FTIR acyl chain (ν-CH_2) stretching peak (~2850 cm^{-1}) during the sol–gel transition.

Measurements of metabolic activity and lactate dehydrogenase (LDH) leakage

Metabolic activity (MA) of the free and encapsulated cells was measured using AlamarBlue (AB) fluorescence.[36] Fluorescence measurements were conducted with a microplate reader (Molecular Devices, Sunnyvale, CA). The samples were excited at 540 nm and emission was measured at 590 nm. MA was measured at 12 h or 24 h of the addition of AB to the encapsulated cells. LDH assay was performed 24 h after immobilization using a commercially available kit (Roche Applied Science, Indianapolis, IN). The levels of extracellular LDH activity were determined by absorbance at 492 nm, using a UV-vis microplate reader (Molecular Devices, Sunnyvale, CA). All measurements were calibrated using blank wells, wells that only contained media, un-encapsulated free cells suspended in media, and silica gels without cells.

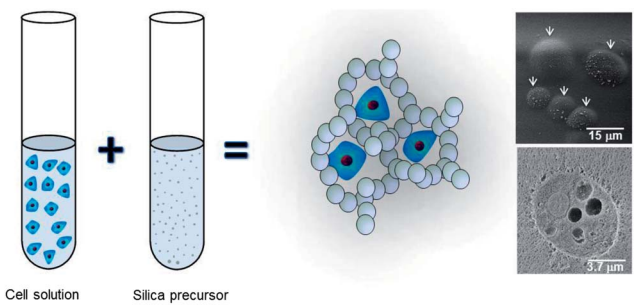

Fig. 1 Cell immobilization process. Cells are suspended in culture media. In a separate container silica precursor and additives are prepared (*e.g.*, THEOS, silica nanoparticles, and PEG). The cell solution and the precursors are then mixed and gelation was achieved within minutes. A 3D nanoporous silica gel surrounded and encapsulated the cells as illustrated in the cartoon and as shown in the electron microscopy images. Top image: white arrows show encapsulated cells right underneath the surface of the gel. Bottom image: cross section of a gel and an encapsulated cell.

Results

HFF and MEF cells were immobilized in pre-granulated THEOS and THEOS–PEG gels that completely encapsulated the cells in a 3D porous gel (Fig. 1). As shown by the SEM images, most cells were encapsulated individually (not in clumps) and remained intact when encapsulated.

Characterization of the pure silica and SPEG gels

Gelation times (T_g) depended on the initial concentration of THEOS in the solution. As the concentration of THEOS increased, T_g decreased resulting in faster gelation (Fig. 2A). This was expected since THEOS acts like a cross-linker binding the SNPs together during gel formation. When PEG was added to silica (SPEG gels), T_g increased with increasing PEG concentration (Fig. 2B). This was expected as well; PEG interacted with the SNPs and THEOS slowing down the gelation kinetics. For SPEG-4arm gels, phase separation was observed at PEG concentrations of 4.5% or below however, gel formation was observed nevertheless. On the other hand, the linear PEGs did not cause phase separation at any concentration used in this study (Fig. S2†). After gel formation, the gels continued to undergo minor structural changes (aging) typical of sol–gel materials. Aging could be observed through the ongoing evolution of the storage (G') and loss (G'') moduli of the pure silica and the SPEG gels (Fig. 2C).

By changing PEG concentration (in the SPEG gels), gel pore size could be tuned (Fig. 2D and E). This enabled tight immobilization of the mammalian cells in a highly porous matrix while minimizing the risk of accidental release from the gel. Fig. 2D shows high magnification SEM images of the silica gel wall (from left to right) in pure THEOS, and in 0.4, 0.6 kDa SPEG-l, and 2 kDa SPEG-4arm gels. All images showed that the backbone of the gels was formed by the aggregation of SNPs in a three dimensional network. The silica gels that did not contain PEG formed a more compact network with much less void space when compared to the SPEG gels. Greater PEG molecular size resulted in higher apparent porosity and void space fraction (Fig. 2E).

The IR spectra obtained from silica and SPEG gels in the 3900–2500 cm^{-1} range were compared. In the pure silica gels, at 3737 cm^{-1} a sharp peak (peak O in Fig. 3A), which corresponded to the stretching vibrations of the unbound silanol groups (–SiOH) on the silica surface was apparent.[37] Moreover, at 3662 cm^{-1} a shoulder (shoulder P in Fig. 3A) originating from the stretching vibrations of the vicinal silanol groups was identified.[37] In SPEG gels both of these silanol peaks disappeared as a

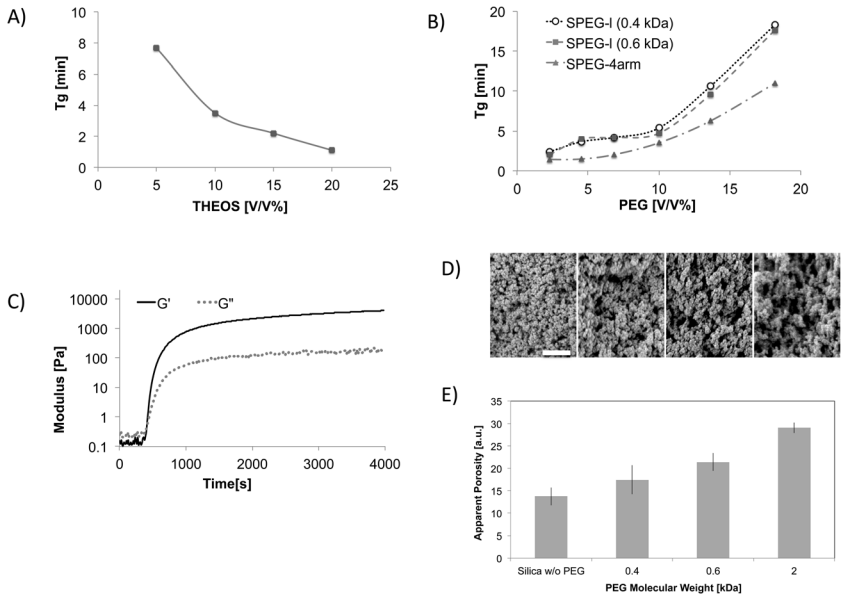

Fig. 2 (A) Gelation time (T_g) of silica gels as a function of THEOS concentration. (B) Gelation time of SPEG gels with PEG molecular weight and concentration. (C) Measurement of gelation kinetics using oscillatory rheometry. The crossover of the storage (G') and loss (G'') moduli measurements represents the onset of gel formation. Note that the measured values keep on evolving beyond the gelation point (this is called aging). (D) Scanning electron microscopy images of different gels. From left to right: silica gel, and SPEG gels with increasing PEG size. The bar represents 500 nm. (E) Apparent porosity of the gel wall structure with changing PEG molecular weight.

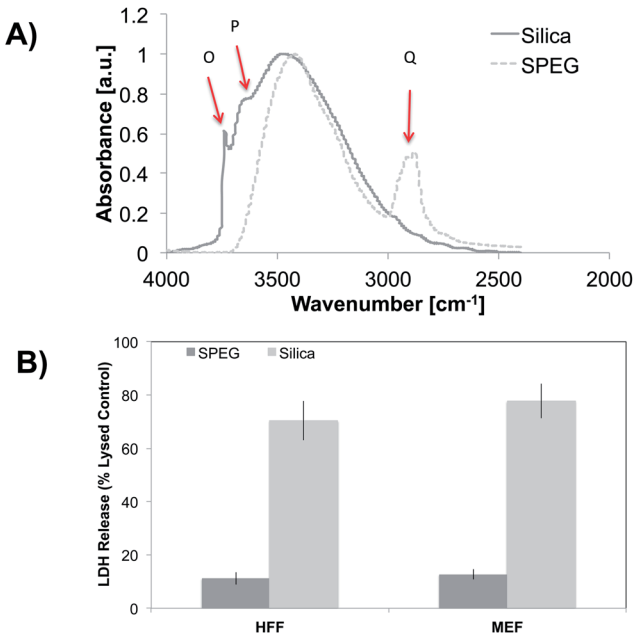

Fig. 3 (A) FTIR spectra in the 2500–4000 cm^{-1} wavenumber region from silica and SPEG gels. (B) LDH release from HFF and MEF cells encapsulated in silica and silica–PEG (10% 4arm-2 kDa PEG) gels after 24 h of immobilization. Values are given as percentage of ethanol lysed control cells.

result of the specific interaction of the PEG with the silica surface groups. A similar behavior was previously reported to happen in colloidal silica suspensions in the presence of organic polymers and sugars.[38,39] In SPEG gels, the asymmetric stretching vibrations (ν-CH_2) of PEG were apparent in the 2900–2750 cm^{-1} region (peak Q in Fig. 3A).

Immobilization in gels

Complete immobilization of the cells within the matrix was confirmed by fluorescence microscopy examination of fluorescently labeled cells (CellTracker™ by Molecular Probes Inc. Eugene, OR) over time and before/after cell counts in selected gels (results not shown here).

Detrimental surface interactions between the cell membrane and the silanol groups were observed by measuring the LDH leakage from the encapsulated cells after 24 h (Fig. 3B). The amount of LDH leakage is known to be proportional to the number of damaged and lysed cells.[40] The LDH leakage study showed that only 11.2% of the HFFs encapsulated in SPEG-4-arm gels were damaged. The damage was confined to 13.5% of the MEF cells encapsulated in similar gels. However, more than 70% of the HFF and MEF cells encapsulated in pure silica gels were damaged. Together with the IR spectra, the LDH test results confirmed that the detrimental effects that bare silica surfaces have on encapsulated cells could be inhibited by PEG.

The protective effect of PEG was further proven when the MA of the encapsulated cells was measured after 24 hours. The results showed that the MA of the encapsulated cells varied with the size and concentration of the PEG used in the gel synthesis (Fig. 4A and B). Cells encapsulated in SPEG-l (0.4 kDa, and 2.3%) had the greatest decrease in MA, dropping within 24 hours down to <15% of the initial value for both HFF and MEF cells. In contrast, cells encapsulated in SPEG-l (0.4 kDa) gels that contained 4.5% and 10% PEG exhibited gradually higher MA ($p > 0.05$). HFF and MEF cells encapsulated in SPEG-l

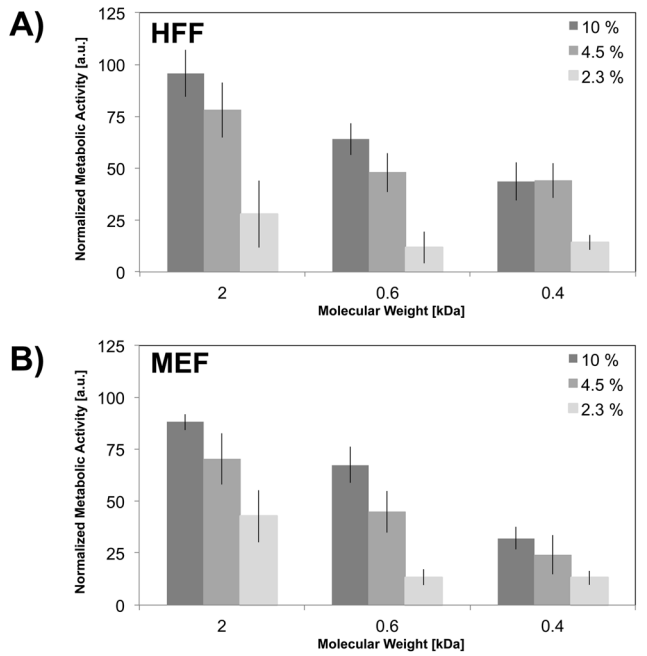

Fig. 4 Effect of PEG concentration and molecular weight on the metabolic activity (MA) of the encapsulated (A) HFF, and (B) MEF cells. MA of encapsulated cells was measured using AlamarBlue assay and normalized with respect to the MA of the free cells growing in incubation medium.

(0.6 kDa) and SPEG-4arm showed the similar dependence of MA on the concentration of PEG used, with higher concentrations of PEG resulted in higher MA. The best results were obtained with SPEG-4arm gels where at 10% PEG concentration the MA of the immobilized HFF and the MEF cells were approximately 96% and 88%, respectively.

As the 10% SPEG-4arm gels resulted in the highest MA, we have focused on these gels for the rest of the studies. After immobilization in pure silica gels, HFF cells experienced an immediate drop of 5.3% ($p < 0.05$) in their MA compared to free cells in media (positive control) (Fig. 5A). For MEFs, the decrease in MA was very significant at over 70% ($p < 0.05$) (Fig. 5B). Within 12 h of immobilization, HFF cells have experienced ~50% decrease of in MA, while the MEF cells lost almost all activity. Within 36 hours, the MA of the pure silica immobilized HFF cells dropped to zero as well.

FTIR analysis showed that the increased viscosity during the sol–gel transition in pure silica gels resulted in an increase in the packing of the cellular membranes, which was evidenced by a decrease in the ν-CH_2 wavenumber by 7.8 cm^{-1} and 8.8 cm^{-1} for HFF and MEF cells, respectively (Table S1†) The changes in the wavenumber did not seem to have a significant immediate effect on the membrane integrity of the encapsulated cells since the membrane integrity of the encapsulated HFF and MEF cells were measured to be 98.3% and 97.3%, (using H & PI fluorescence) immediately after immobilization. However, over time, specific surface interactions at the silica lipid interface potentially caused disruption in the cellular membranes as indicated by the large release of LDH from the cytoplasm of encapsulated HFF and MEF cells (Fig. 3B).

Incorporation of 10% 4-arm PEG into the immobilization matrix had a very positive effect on the MA of the encapsulated cells. HFF and MEF cells still showed approximately 77% and 46% of the free cell MA, respectively after 24 h of immobilization (Fig. 5A and B). However, the decrease in MA over time could not be fully stopped and after 60 hours reached that measured in the negative control values.

Additionally, the effect of arresting cellular division was examined. HFFIR and MEFIR cells were metabolically more active when compared to the HFF and MEF cells at all time-points (Fig. 5C and D). Interestingly, the MA of the encapsulated irradiated cells were even higher than that of free cells (the positive control) for as long as 48 hours. After 60 h of immobilization, the MA of HFFIR and MEFIR cells were less than 50% and the MA values decreased to the levels of negative controls by 84 h of immobilization (data not shown).

Immobilization and release of mammalian cells from granulated pure silica and SPEG gels

After 24 hours of immobilization approximately 55.0 ± 15.8% of the cells encapsulated in granulated SPEG gels could be recovered compared to only 14.5% ± 9.9 recovered from the granulated pure silica gels. It is noteworthy that the extracted cells could proliferate normally when incubated under normal conditions after extraction (Table 1).

Discussion

We have identified four major factors that have contributed to the long-term survival of encapsulated eukaryotes inhibited from growth, migration and proliferation:

(1) *Porosity/permeability of the gel*: large organic molecules such as albumin, gelatin and casein can be combined with THEOS to produce porous networks.[41] Cell growth medium also contains large biomolecules such as growth factors and albumin and therefore even pure THEOS gels prepared in this study in cell growth media was highly porous (Fig. 2D). The SEM images showed that the silica gels were formed by the three dimensional aggregation of SNPs with a random distribution of pores (Fig. 2D). When PEG was incorporated into the silica sol, an increase in the porosity of the resultant gel was observed. The increase in porosity was proportional to the molecular weight of the PEG added (Fig. 2E). Note that, even in the most porous gels used in this study the pore size was in the order of tens of nanometers and therefore was still not large enough to allow cellular motility, growth or proliferation. It is also highly likely that the porosity of the gel was not high enough to allow easy diffusion of large biomolecules (such as growth factors) into the gel, inducing a condition of partial starvation for the immobilized cells. This is considered an important factor limiting the viability of the silica gel immobilized cells.

(2) *Structural homogeneity of the gel*: it was shown that the concentration of PEG in the gel was critical. Depending on the type and concentration of PEG used in the gel, phase separation

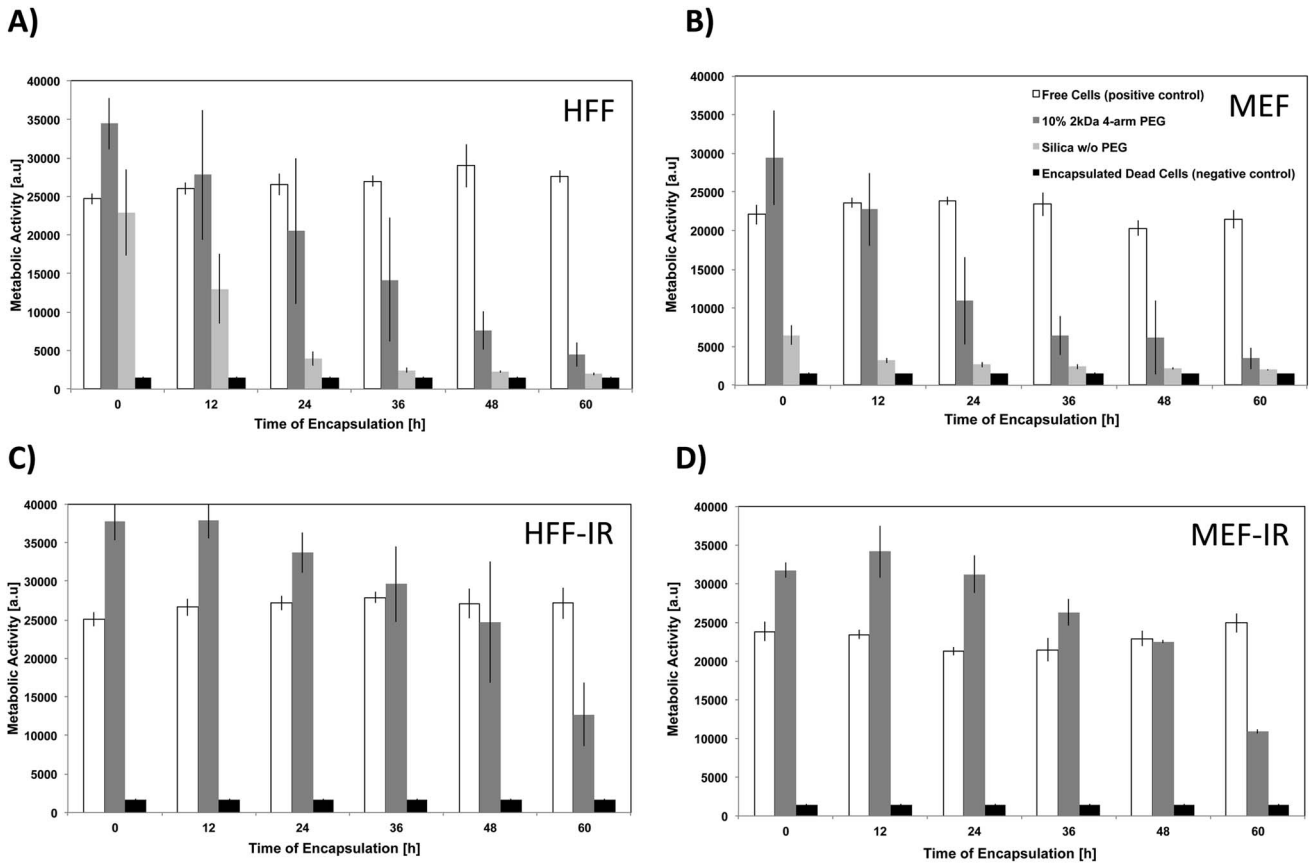

Fig. 5 Metabolic activity of the silica and silica–PEG encapsulated cells; (A) HFF, (B) MEF, (C) irradiated HFF, and (D) irradiated MEF cells. Negative controls (black) were prepared by encapsulating dead HFF and MEF cells. Free cells incubated in growth medium were used as the positive control.

Table 1 Proliferation of cells after extraction

		Doubling time [days]
Free cells	2000 cells[a]	1.41 ± 0.06
	5000 cells[a]	1.57 ± 0.13
	10 000 cells[a]	1.35 ± 0.10
Cells released after immobilization for 24 hours	Cells[b] released from 10% SPEG gel (granulated)	2.01 ± 0.91
	Cells[b] released from 0% SPEG gel (granulated)	1.37 ± 0.25

[a] Total cells in T75 flask. [b] Approximately between 10–20k cells in a T75 flask.

occurred (Fig. S2B and C†). In the extreme cases (*e.g.* low concentrations of 2 kDa 4-arm PEG), phase separation could even be detected visually (Fig. S2A†), and resulted in a mechanically weak and compositionally heterogeneous gel. In general, higher concentrations of PEG resulted in a more homogeneous gel. Therefore, structural homogeneity of the resultant gel was considered to be another factor that contributed to the viability of immobilized cells (Fig. 4).

(3) *Specific interactions of the cell membrane with the gel surface*: it was shown that PEG also formed a buffer region between the cell membrane and the surface groups of the silica gel by establishing strong hydrogen bonds with the silanol groups of the silica matrix. This was confirmed by FTIR analysis of the gel (Fig. 3A).[42] It is also known that *trans*-esterification reactions between hydrolyzed alkoxides and PEG might take place during sol–gel processing,[43] resulting in covalent interactions between PEG and silica reactive group as shown by NMR spectroscopy and differential scanning calorimetry studies conducted by others.[43,44] The buffer zone decreased the harmful interactions between the encapsulated cells and the silica surface, decreasing the LDH release from the cells (Fig. 3B) and very significantly increasing the survival of the immobilized cells (Fig. 5).

The significant structural changes the cell membranes experienced after immobilization in pure silica gels was also evidenced by the FTIR studies conducted here (Table S1†). The membranes of cells in solution are in a liquid-crystalline state (with a ν-CH_2 peak position of approximately 2852 cm^{-1}). At the liquid crystalline state, lipid head group spacing is high, the acyl chains are disordered and the lipid bilayer thickness is low.[45] It was observed that silica gelation was accompanied by an abrupt decrease in the ν-CH_2 wavenumber (Table S1†), showing a more gel-like transition of the immobilized cell membrane. In the gel phase, the membrane lipid acyl chains

are ordered, the lipid head groups are packed closely and the overall permeability of the lipid bilayer therefore decreases.[46] However, the overall membrane structure may become leakier due to defect formation at phase boundaries.[47–49] Increased packing of the membrane lipids upon silica gel encapsulation was previously reported for prokaryotic cells.[50] It is highly likely that these stresses on the membrane caused the increased leaking of LDH observed in pure silica gels (Fig. 3B). Specific interactions between the silica surface and the immobilized cell membrane are therefore determined to be another very important factor in long-term encapsulated cell viability.

One shortcoming of the FTIR study presented here is that the positive effect of the presence of PEG on the encapsulated cell membrane structure could not be directly shown using the ν-CH_2 spectra since these bands are masked by very dominant PEG bands.

(4) *Proliferation stress*: in this study, the encapsulated cells were immobilized in a mechanically stiff cell where they could not migrate, grow or proliferate. We have hypothesized that this would generate a significant source of stress. It is highly likely that the encapsulated cells have been following a normal cell cycle, eventually ending in mitosis. However, the tight confinement of the cell within the gel (Fig. 1) would not allow cell division (Fig. S3†).[51] The HFF and MEF cells were therefore irradiated before encapsulation – to stop mitosis – to examine the effect of proliferation stress. It was shown conclusively that when irradiated, the survival of the cells immobilized in silica gels increased very significantly. For example, both the irradiated HFF cells (HFF-IR) and the irradiated MEF cells were as metabolically active as the free control cells grown in media for up to 48 hours (Fig. 5A and B).

These results not only showed that the proliferative stress was an important factor in determining the survival of encapsulated cells but also opened up very novel avenues for exploration: for example, the immobilization gel and the methodology developed here can be used to distinguish between normal and cancerous cell types with significantly different growth rates, doubling times and ability to transition into dormancy.

Conclusion

We have used pre-granulated THEOS-based PEG gels stiff enough to immobilize encapsulated mammalian cells and inhibit their growth, migration and proliferation. Four main factors were identified to determine the long-term survival within the immobilization gels: (1) porosity/permeability of the gel, (2) structural homogeneity of the gel, (3) specific interactions between the cell membrane and the gel surface and (4) the proliferative stress. It was further shown that the immobilized cells could easily be mechanically recovered from the gel and upon incubation, proliferated normally (Table 1).

Acknowledgements

This research was supported by a National Science Foundation grant (CBET-0644784).

References

1 V. Nedovic and R. Willaert, *Fundamentals of Cell Immobilization Biotechnology*, Klumer Academic Publishers, Dordrecht, 2004.
2 J. W. Haycock, *3d Cell Culture*, 2011.
3 G. Orive, A. R. Gascon, R. M. Hernandez, M. Igartua and J. L. Pedraz, Cell Microencapsulation Technology for Biomedical Purposes: Novel Insights and Challenges, *Trends Pharmacol. Sci.*, 2003, **24**, 207–210.
4 G. Orive, R. M. Hernandez, A. R. Gascon and J. L. Pedraz, Biomedical Applications of Immobilaized Cells, in *Immobilization of Enzymes and Cells*, ed. J. M. Guisan, Human Press Inc., 2006.
5 T. M. S. Chang, Therapeutic Applications of Polymeric Artificial Cells, *Nat. Rev. Drug Discovery*, 2005, **4**, 221–234.
6 A. Murua, A. Portero, G. Orive, R. Hernández, M. d. Castro and J. L. Pedraz, Cell Microencapsulation Technology: Towards Clinical Application, *J. Controlled Release*, 2008, **132**, 76–83.
7 P. DeVos, B. J. DeHaan, G. H. J. Wolters, J. H. Strubbe and R. VanSchilfgaarde, Improved Biocompatibility but Limited Graft Survival after Purification of Alginate for Microencapsulation of Pancreatic Islets, *Diabetologia*, 1997, **40**, 262–270.
8 M. B. Aydelotte, E. Thonar, J. Mollenhauer and J. Flechtenmacher, Culture of Chondrocytes in Alginate Gel: Variations in Conditions of Gelation Influence the Structure of the Alginate Gel, and the Arrangement and Morphology of Proliferating Chondrocytes, *In Vitro Cell. Dev. Biol.: Anim.*, 1998, **34**, 123–130.
9 C. F. Meunier, P. Dandoy and B.-L. Su, Encapsulation of Cells within Silica Matrices: Towards a New Advance in the Conception of Living Hybrid Materials, *J. Colloid Interface Sci.*, 2009, **342**, 211–224.
10 M. Blondeau and T. Coradin, Living Materials from Sol–Gel Chemistry: Current Challenges and Perspectives, *J. Mater. Chem.*, 2012, **22**, 22335–22343.
11 D. Avnir, T. Coradin, O. Lev and J. Livage, Recent Bio-Applications of Sol–Gel Materials, *J. Mater. Chem.*, 2006, **16**, 1013–1030.
12 J. R. Premkumar, E. Sagi, R. Rozen, S. elkin, A. D. Modestov and O. Lev, Fluorescent Bacteria Encapsulated in Sol–Gel Derived Silicate Films, *Chem. Mater.*, 2002, **14**, 2676–2686.
13 J. R. Premkumar, R. Rosen, S. Belkin and O. Lev, Sol–Gel Luminiscence Biosensor: Encapsulation of Recombiant *E. coli* Reporters in Thick Silicate Films, *Anal. Chim. Acta*, 2002, **462**, 11–23.
14 A. Leonard, P. Dandoy, E. Danloy, G. Leroux, C. F. Meunier, J. C. Rooke and B.-L. Su, Whole-Cell Based Hybrid Materials for Green Energy Production, Environmental Remediation and Smart Cell Theraphy, *Chem. Soc. Rev.*, 2011, **40**, 860–885.
15 U. Soltmann, S. Mayts, G. Kieszig, W. Pompe and H. Bottcher, Algae–Silica Hybrid Materials for Biosorption of Heavy Metals, *J. Water Resour. Prot.*, 2010, **2**, 115–122.

16 I. Kaur, A. K. Bhatnagar, S. Ved Pal and D. Stapleton Raymond Jr, Algae-Dependent Bioremediation of Hazardous Wastes, in *Progress in Industrial Microbiology*, Elsevier, 2002, vol. 36, pp. 457–516.

17 J. C. Rooke, A. Leonard, H. Sarmento, C. F. Meunier, J. P. Descy and B. L. Su, Novel Photosyntheic CO_2 Bioconvertor Based on Green Algae Entrapped in Low-Sodium Silcia Gels, *J. Mater. Chem.*, 2011, **21**, 951–959.

18 D. J. Dickson and R. L. Ely, Evaluation of Encapsulation Stress and the Effect of Additives on the Viabiliaty and Photosynthetic Activity of Synechocystis Sp. Pcc 6803 Encapsulated in Silica Gel, *Appl. Microbiol. Biotechnol.*, 2011, **91**, 1633–1646.

19 P. Dandoy, C. F. Meunier, C. Michiels and B. L. Su, Hybrid Shell Engineering of Animal Cells for Immune Protections and Regulation of Drug Delivery: Towards the Design of "Artificial Organs", *PLoS One*, 2011, **6**, e20983.

20 D. B. Jaroch, J. Lu, R. Madangopal, N. D. Stull, M. Stensberg, J. Shi, J. L. Kahn, R. Herrera-Perez, M. Zeitchek, J. Sturgis, J. P. Robinson, M. C. Yoder, D. M. Porterfield, R. G. Mirmira and A. J. L. Rickus, Mouse and Human Islets Survive and Function after Coating by Biosilicification, *Am. J. Physiol.: Endocrinol. Metab.*, 2013, **305**, E1230–E1240.

21 P. N. Catalano, N. S. Bourguignon, G. S. Alvarez, A. Carlos Libertun, L. E. Diaz, M. F. Desimone and V. Lux-Lantosa, Sol–Gel Immobilized Ovarian Follicles: Collaboration between Two Different Cell Types in Hormone Production and Secretion., *J. Mater. Chem.*, 2012, **22**, 11681–11687.

22 E. J. A. Pope, K. Braun and C. M. Peterson, Bioartificial Organs I: Silica Gel Encapsulated Pancreatic Islets for the Diabetes Mellitus, *J. Sol-Gel Sci. Technol.*, 1997, **8**, 635–639.

23 G. Carturan, R. Dal Toso, S. Boninsegna and R. Dal Monte, Encapsulation of Functional Cells by Sol–Gel Silica: Actual Progress and Perspectives for Cell Therapy, *J. Mater. Chem.*, 2004, **14**, 2087–2098.

24 S. Boninsegna, P. Bosetti, G. Carturan, G. Dellagiacoma, R. Dal Monte and M. Rossi, Encapsulation of Individual Pancreatic Islets by Sol–Gel SiO_2: A Novel Procedure for Perspective Cellular Grafts, *J. Biotechnol.*, 2003, **100**, 277–286.

25 G. Carturan, G. Dellagiacoma, M. Rossi, R. Dal Monte and M. Muraca, in *Encapsulation of Viable Animal Cells for Hybrid Bioartificial Organs by the Biosil Method*, 1997, pp. 366–373.

26 A. Nieto, S. Areva, T. Wilson, R. Viitala and M. Vallet-Regi, Cell Viability in a Wet Silica Gel, *Acta Biomater.*, 2009, **5**, 3478–3487.

27 M. A. Snyder, D. Demirgoz, E. Kokkoli and M. Tsapatsis, Benign, 3d Encapsulation of Sensitive Mammalian Cells in Porous Silica Gels Formed by Lys-Sil Nanoparticles Assembly, *Microporous Mesoporous Mater.*, 2009, **118**, 387–395.

28 M. F. Desimone, M. C. D. Marzi, G. S. Alvarez, I. Mathov, L. E. Diaz and E. L. Malchiodix, Production of Monoclonal Antibodies from Hybridoma Cells Immobilized in 3d Sol–Gel Silica Matrices, *J. Mater. Chem.*, 2011, **21**, 13865–13872.

29 S. Sakai, T. Ono, H. Ijima and K. Kawakami, Min6 Cells-Enclosing Aminopropyl-Silicate Membrane Templated by Alginate Gels Differences in Guluronic Acid Content, *Int. J. Pharm.*, 2004, **270**, 65–73.

30 S. Sakai, T. Ono, H. Ijima and K. Kawakami, Proliferation and Insulin Secretion Functional of Mouse Insulinoma Cells Encapsulated in Alginate/Sol–Gel Synthesis Aminopropyl-Silicate/Alginate Microcapsule, *J. Sol-Gel Sci. Technol.*, 2003, **28**, 267–272.

31 J. C. Harper, D. M. Lopez, E. C. Larkin, M. K. Economides, S. K. McIntyre, T. M. Alam, M. S. Tartis, M. Werner-Washburne, C. J. Brinker, S. M. Brozik and D. R. Wheeler, Encapsulation of *S. cerevisiae* in Poly(Glycerol) Silicate Derived Matrices: Effect of Matrix Additives and Cell Metabolic Phase on Long-Term Viability and Rate of Gene Expression, *Chem. Mater.*, 2011, **23**, 2555–2564.

32 N. Nassif, A. Coiffier, T. Corandin, C. Roux and J. Livage, Viability of Bacteria in Hybrid Aqueous Silica Gels, *J. Sol-Gel Sci. Technol.*, 2003, **26**, 1141–1144.

33 L. Inama, S. Diré and G. Carturan, Entrapment of Viable Microorganisms by SiO_2 Sol–Gel Layers on Glass Surfaces: Trapping, Catalytic Performance and Immobilization Durability of *Saccharomyces cerevisiae*, *J. Biotechnol.*, 1993, **30**, 197–210.

34 M. D. Abramoff, P. J. Magalhaes and S. J. Ram, *Image Processing with ImageJ. Biophotonics International*, 2004, vol. 11, pp. 36–42.

35 W. S. Rasband, *ImajeJ*, U.S. National Institute of Health, Bethesda, Maryland, USA, 1997.

36 R. D. Fields and M. V. Lancaster, Dual-Attribute Continuous Monitoring of Cell Proliferation/Cytotoxicity, *Am. Biotechnol. Lab.*, 1993, **11**, 48–50.

37 K. M. Davis and M. Tomozawa, An Infrared Spectroscopy Study of Water-Related Species in Silica Glasses, *J. Non-Cryst. Solids*, 1996, **201**, 177–198.

38 J. Rubio and J. A. Kitchener, The Mechanism of Adsorption of Poly(Ethylene Oxide) Flocculant on Silica, *J. Colloid Interface Sci.*, 1976, **57**, 132–142.

39 E. Reátegui and A. Aksan, Effects of Water on the Structure and Low/High Temperature Stability of Confined Proteins, *Phys. Chem. Chem. Phys.*, 2010, **12**, 10161–10172.

40 S. F. Khattak, S. R. Bathia and S. C. Roberts, Pluronic F127 as a Cell Encapsulation Material: Utilization of Membrane Stabilizing Agents, *Tissue Eng.*, 2005, **11**, 974–983.

41 Y. Shchipunov and N. Shipunova, Regulation of Silica Morphology by Proteins Serving as a Template for Mineralization, *Colloids Surf., B*, 2008, **63**, 7–11.

42 R. K. Iler, *The Chemistry of Silica: Solubility, Polymerization, Colloid and Surface Properties, and Biochemistry*, John Wiley & Sons, New York, 1979.

43 P. Lesot, S. Chapuis, J. P. Bayle, J. Rault, E. Lafontaine, A. Campero and P. Judeinstein, Structural-Dynamical Relationships in Silica Peg Hybrid Gels, *J. Mater. Chem.*, 1998, **8**, 147–151.

44 M. Stefanescu, M. Stoia and O. Stefasnecu, Thermal and FTIR Study of the Hybrid Ethylene Glycol Silica Matrix, *J. Sol-Gel Sci. Technol.*, 2007, **41**, 71–78.

45 J. F. Nagle, Theory of the Main Lipid Bilayer Phase Transition, *Annu. Rev. Phys. Chem.*, 1980, **31**, 157–196.
46 G. Cevc, Isothermal Lipid Phase Transitions, *Chem. Phys. Lipids*, 1991, **57**, 293–307.
47 G. Cevc, Isothermal Lipid Phase Transitions, *Chem. Phys. Lipids*, 1991, **57**, 293–307.
48 T. H. Haines, Water Transport across Biological-Membranes, *FEBS Lett.*, 1994, **346**, 115–122.
49 D. Papahadjopoulos, K. Jacobson, S. Nir and T. Isca, Phase Transitions in Phospholipid Vesicles, *Biochim. Biophys. Acta*, 1973, **311**, 330–348.
50 E. Reátegui, E. Reynolds, L. Kasinkas, A. Aggarwal, M. Sadowsky, A. Aksan and L. Wackett, Silica Gel-Encapsulated Atza Biocatalyst for Atrazine Biodegradation, *Appl. Microbiol. Biotechnol.*, 2012, **96**, 231–240.
51 T. Branyik, G. Kunkova, J. paca and K. Demnerova, Encapsulation of Microbial Cells into Silica Gels, *J. Sol-Gel Sci. Technol.*, 1998, **13**, 283–287.